International Journal of Advances in Engineering and Management (IJAEM)
Volume 4, Issue 2 Feb 2022, pp: 1397-1412 www.ijaem.net ISSN: 2395-5252

Intelligent High Voltage Direct Current (Ihvdc) Based Transient tability improvementofa Transmission System

Umeozulu Ada S.[1]., Eneh Ifeanyi I..[2],Aneke Jude. I.[3]and AbonyiObianuju D.[4]

[1]*Transmission Company of Nigeria, Enugu, Nigeria,* [2,4]*Enugu State University of Science and Technology, Enugu, Nigeria,* [3]*Nnamdi Azikiwe University, Awka, Nigeria*

Submitted: 15-02-2022 Revised: 25-02-2022 Accepted: 28-02-2022

ABSTRACT-Power system researchers in the past decades have faced a major challenge with the enhancement of the dynamic response of generators within a power system, when subjected to different disturbances. Therefore, using the Nigeria 330kV transmission network as a case study, this paper presents the application of an intelligent VSC-HVDC system for the improvement of the transient stability. At start, eigen value analysis of the system buses was performed to determine the buses that are marginally unstable (critical buses) in the network. Then, a balanced 3-phase fault was applied to the few critical buses and lines of the transmission network. Then, by observing the dynamic response of the generators in the Nigeria 330kV grid, the existing transient stability situation was determined. The finding obtained vividly revealed that buses Omotosho and Shiroro are the two most critical buses while transmission lines from Omotosho - Benin TS and Jebba TS-Shiroro GS within the network are the most critical transmission lines. Also, when the balanced 3-phase fault was applied to these mentioned critical buses and lines, the network loses synchronism. As a solution, VSC-HVDC was installed at the identified lines that are marginally unstable. The artificial neural network (ANN) was used to control the parameters of the VSC-HVDC converter and the converter in MATLAB/PSAT environment. The results obtained showed that the fault critical clearing time (CCT) was increased from 300milli-seconds to 450milli-seconds which is 50% increment. Also, the oscillations were quickly damped compare to the results obtain when the VSC-HVDC was being controlled by the conventional PI method.

I. INTRODUCTION

Nowadays, the demand for electricity has radically increased and a modern power system becomes a difficult network of transmission lines interconnecting the generating stations to the major load centers in the overall power system in order to support the high demand of consumers. Transmission networks being overloaded are pushed closer to their stability limits. This is as a result of increasing demand for electricity due to growing population. This could have negative effect on the power system security. The security of a power system is regarded as the ability of the network to withstand disturbances without breaking down (Karthikeyan and Dhal, 2015). The complicated network causes the stability problem. Stability is determined by the observation of voltage, frequency and rotor angle. One of the indices to assess the state of security of a power system is the transient stability (Ayodele, Ogunjuyigbe and Oladele, 2016) and it involves the ability of power system to remain in equilibrium or return to acceptable equilibrium when subjected to large disturbances (Ayodele, Jimoh, Munda and Agee, 2012). Transient stability examines the impact of disturbance in power systems considering the operating conditions. The analysis of the dynamic behavior of power systems for the transient stability gives information about the ability of power system to sustain synchronism during and after the disturbances.

Fault occurrences in a power system cannot be eliminated; however, its impact which affects the security margins of the network can be reduced. Fault occurrences usually result in the unstable situation in the power network operations. Currently, this issue has become a thing of huge concern to power system engineers and researchers.

International Journal of Advances in Engineering and Management (IJAEM)
Volume 4, Issue 2 Feb 2022, pp: 1397-1412 www.ijaem.net ISSN: 2395-5252

Therefore, to resolve this challenge, efforts should be focused on evaluating the capability and power system response especially when the power system is placed under some faults with the idea of preserving the reliability of the system. Power systems instability can be of different kinds depending on the duration. If a power network is placed under a disturbance, loss of synchronism may occur and this normally leads to an entire collapse of voltage within the system. This clarifies the reason transient stability improvement is of great concern in the power network operation. Different methods of improving a multi-machine power network transient stability have been studied (Srinvasa and Amarnath, 2014). These methods include: the application of fault current limiter (FCL), reducing the network transfer reactance, the FACTS devices placements, the breaking resistor application and the application of bundled conductor (Rani and Arul, 2013).

The controllability of the HVDC power is often used to improve the operating conditions of the AC network where the converter stations are located. HVDC allows more efficient bulk power transfer over distances. However, cost is important variable in the equation. Once installed, HVDC transmission systems are integral part of the electrical power system, improving stability, reliability and transmission capacity. High Voltage Direct Current (HVDC) power transmission is employed to move large amounts of electric power. There are several possibilities to enhance the transient stability in a power system. One adequate option is by using the high controllability of the HVDC if HVDC is available in the system(Hua, Tian-gang, Mu-Zi andZhi-min, 2012). The strategy controls the power through the HVDC to help make the system more transient stable during disturbances. Loss of synchronism is prevented by quickly producing sufficient decelerating energy to counteract accelerating energy gained. The power flow in the HVDC link is modulated with the addition of an auxiliary signal to the current reference of the rectifier firing angle controller. This modulation control signal is derived from speed deviation signal of the generator utilizing a PD controller; the utilization of a PD controller is suitable because it has the property of fast response. It has been demonstrated that the power flow in the HVDC link is modulated by the addition of an auxiliary signal to the current reference of the rectifier firing angle controller to enhance the transient stability in power system. The proportional, integral and derivative (PID) controller works well and damps the first swing oscillation transient so the system remains stable (Eriksson, 2014). Therefore, the control of HVDC has the potential for future application to power systems. The PID controllers has been used in the past for controlling HVDC, however Artificial Intelligent technique like ANN promises to be a more intelligent controller that can achieve better result in transient stability improvement of power system.

II. THE WORKING CONCEPT OF HVDC TRANSMISSION SYSTEM

In generating substation, AC power is produced which can be changed over into DC by utilizing a rectifier. In HVDC substation or converter substation rectifiers and inverters are set up at both the closures of a line as shown in Figure 1. The rectifier terminal changes the AC to DC, while the inverter terminal converts DC to AC. The DC is streamed through the overhead lines and at the client end again DC is changed over into AC by utilizing inverters, which are put in converter substation(Mohapatra, 2015). The power stays as before at the sending, upon getting to the receiving end. DC is transferred over significant distances since it diminishes the losses and enhances the efficiency.

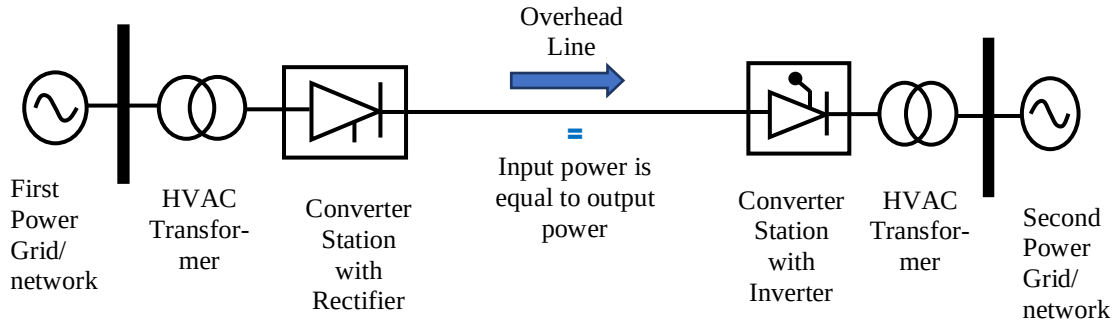

Figure 1:HVDC Substation Layout.

International Journal of Advances in Engineering and Management (IJAEM)
Volume 4, Issue 2 Feb 2022, pp: 1397-1412 www.ijaem.net ISSN: 2395-5252

III. DETERMINATION OF THE TRANSIENT STABILITY OF THE NIGERIA 330KV NETWORK AND THE WEAKEST BUSES

The aim here is to determine the system buses that are most marginally unstable. To ensure that the buses to be used are marginally unstable, the buses selected are buses having eigenvalue that lie on the right side of the S-plane and having lowest value of damping ratio. By clicking on the eigenvalue analysis button on the PSAT, the transient stability of the network was analyzed from the result obtained. The output from the eigenvalue analysis by the PSAT model of the Nigeria 330kV transmission grid was extracted and tabulated in Table 1.

3.1 Mathematical Derivation of Swing Equation for a Multi- Machine Power System

If we consider a multi-machine n-bus power network consisting of m number of generators such that n >m. Then at any bus I within the network, the complex voltages (V_i), real power of the generator (P_{gi}) and the reactive power of the generator(Q_{gi}) can simply be gotten from the pre-fault load-flow analysis from which the initial machine voltages (E_i) can also be gotten. This relationship can be communicated as (Sravani, Hari, and Basha, 2010):

$$E_i = V_i + jX_i\left[\frac{P_{gi} - jQ_{gi}}{V_i^*}\right] \quad (1)$$

where;

X_i is the equivalent reactance at bus i. By transforming each load bus into its equivalent constant admittance form, we have

$$Y_{Li} = \frac{P_{Li} - jQ_{Li}}{|V_i|^2} \quad (2)$$

Where P_{Li} and Q_{Li} are the equivalent real and reactive powers respectively at each load buses. The pre-fault bus admittance matrix [bus Y] can therefore be formed with the inclusion of generators reactance and the converted load admittance. This can be partitioned as (Sravani, Hari, and Basha, 2010):

$$Y_{bus} = \begin{bmatrix} Y_{11} & Y_{12} \\ Y_{21} & Y_{22} \end{bmatrix} \quad (3)$$

Where Y_{11}, Y_{12}, Y_{21}, and Y_{22} are the sub-matrices of Y_{bus}. Out of these four sub-matrices, Y_{11}, whose dimension is $m \times m$ is the primary interest here as it contains generators buses just with the load buses disposed of. Equation (3) is formulated for the system states such as pre-fault, during fault and post-fault. The bus Y for the system is then derived by disposing all nodes except the internal generator nodes. The decrease is accomplished dependent on the fact that injections at all load nodes are zero. The nodal equations, in smaller form, can thusly be communicated as (Sharma, and Hooda, 2012):

$$\begin{bmatrix} 1 \\ 0 \end{bmatrix} = \begin{bmatrix} Y_{mm} & Y_{mn} \\ Y_{nm} & Y_{nn} \end{bmatrix}\begin{bmatrix} V_m \\ V_n \end{bmatrix} \quad (4)$$

By expansion equation (3.4) can be expanded as

$$I_m = Y_{mm}V_m + Y_{mn}V_n \quad (5)$$

and

$$0 = Y_{nm}V_m + Y_{nn}V_n \quad (6)$$

By combining equations (5) and (6) and some mathematical manipulations, the desired reduced admittance matrix can be obtained as

$$Y_{reduced} = Y_{mm} - Y_{mn}Y_{nn}^{-1}Y_{nm} \quad (7)$$

$Y_{reduced}$ is the desired reduced matrix with dimension m x m, where m is the number of generators. The output power of each machine can then be stated as (Machowski, Kacejko, Nogal and Wancerz 2013):

$$P_{ei} = E_i^2 Y_{ii}\cos\theta_{ii} + \sum_{\substack{i=1 \\ j\neq 1}}^{m} |E_i||E_j||Y_{ij}|\cos\left(\theta_{ij} - \delta_i + \delta_j\right) \quad (8)$$

Equation (3.8) can then be employed to calculate the system during fault $P_{ei}(P_{ei(during\ -fault\ )})$ and post-fault $P_{ei}(P_{ei(post\ -fault\ )})$ conditions.The rotor dynamics, representing the swing equation, at any bus i, is written by (Sharma, and Hooda, 2012):

$$\frac{H_i}{\pi f_0}\frac{d^2\delta_i}{dt^2} + D_i\frac{d_i}{dt} = P_{mi} - P_{ei} \quad (9)$$

All the parameters assume their normal meanings.If we examine a case when there is no damping, that is $D_i = 0$, equation (9) can be transformed as

International Journal of Advances in Engineering and Management (IJAEM)
Volume 4, Issue 2 Feb 2022, pp: 1397-1412 www.ijaem.net ISSN: 2395-5252

$$\frac{H_i}{\pi f_0}\frac{d^2\delta_i}{dt^2} = P_{mi} - \left(E_i^2 Y_{ii}\cos\theta_{ii} + \sum_{\substack{j=1 \\ j\neq 1}}^{m} |E_i||E_j||Y_{ij}|\cos(\theta_{ij} - \delta i + \delta j \quad (10)$$

The swing equation for the during-fault condition can simply be communicated as

$$\frac{H_i}{\pi f_0}\frac{d^2\delta_i}{dt^2} + D_i\frac{d_i}{dt} = P_{mi} - P_{ei(during\ -fault\ )} \quad (11)$$

Similarly, the swing equation for the post fault condition can also be communicated as

$$\frac{H_i}{\pi f_0}\frac{d^2\delta_i}{dt^2} + D_i\frac{d_i}{dt} = P_{mi} - P_{ei(post\ -fault\ )} \quad (12)$$

3.2 Eigen value Analysis

The Eigen value analysis investigates the dynamic behavior of a power system under different characteristic frequencies (''modes''). In a power system, it is required that all modes are stable. Moreover, it is desired that all electromechanical oscillations are damped out as quickly as possible. The Eigen value (γ) gives information about the proximity of the system to instability. The participation factor measures the participation of a state variable in a certain mode oscillation (Eleschová, Smitková and Beláň, 2010). The damping ratio (τ) is an indication of the ability of the system to return to stable state in the event of disturbance.

The case study network (the existing Nigeria 40 bus 330kV transmission grid) was designed in MATLAB/PSAT environment and simulation procedure and results specific to its parameters were obtained. This enabled this paper to explore the peculiarity of the Nigerian power system.Table 1shows the output from the Eigen value analysis on the PSAT model of the Nigeria 330kV transmission grid.It can be seen that the network is generally not stable.

This is due to the fact that all the Eigen values are not located on the left side of the S-plane. The Eigen values located on the left side of the S-plane are negative (stable) whereas Eigen values located on the right side of the S-plane are positive (unstable). However, not all the buses in the power system are part of the instability. Among all the buses whose Eigen values are located on the right side of the S-plane, the most unstable buses would be selected for application of three phase fault for the evaluation of the system transient stability improvement using ANN controlled VSC-HVDC. The buses located on the right side of the S-plane are unstable buses but since two buses are to be selected, the damping ratio is used as the criterion for the selection. The lower the damping ratio, the more unstable the bus would be.From the Table 1, the buses selected are Omotosho – bus 33 and Shiroro - bus 38. The Eigen values of these buses are $2.7297 \pm j5.5635$ and $0.1674 \pm j4.1170$ with damping ratios of 0.0384 and 0.0251 respectively. The eigenvalues of these buses are located on the right side of the S-plane and they are the buses with the lowest damping ratio. These selected buses 33 and 38 were now subjected to a three phase faults one after the other whereas the loads at buses were held constant at the demand values.

Table 1: Extracted output from Eigen value analysis in PSAT environment

Bus Number	Bus Name	Eigen Value (γ)	Damping Ratio (τ)	Participation Factor (%)
1	AES	$1.7653 \pm j10.4192$	0.4427	2.2076
2	Afam	$-1.7011 \pm j3.1375$	0.3442	0.0768
3	Aja	$-2.1746 \pm j6.7011$	0.2632	0.7139
4	Ajaokuta	$-1.9640 \pm j5.3208$	0.6412	2.6122
5	Akangba	$2.0367 \pm j8.2287$	0.5941	0.6122
6	Aladja	$-3.4083 \pm j7.5374$	0.7456	2.4165
7	Alagbon	$0.2562 \pm j5.7324$	0.6745	0.4165
8	Alaoji	$-0.4528 \pm j4.2183$	0.6259	1.0817
9	Ayiede	$-2.7653 \pm$ j11.2419	0.4933	0.3021
10	Benin	$1.7301 \pm$ j3.1375	0.2193	3.3021
11	Brenin Kebbi	$-2.1674 \pm$ j5.1101	1.3511	0.3228

International Journal of Advances in Engineering and Management (IJAEM)
Volume 4, Issue 2 Feb 2022, pp: 1397-1412 www.ijaem.net ISSN: 2395-5252

12	Damaturu	$1.6064 \pm j6.8320$	0.8232	3.1297
13	Delta	$-2.0367 \pm j8.2287$	0.7624	1.1096
14	Egbin	$3.4083 \pm j7.5374$	0.8320	0.3176
15	Ganmo	$-0.2562 \pm j5.7324$	0.8031	0.2113
16	Geregui	$-0.4528 \pm j4.2183$	0.2803	0.2113
17	Gombe	$-4.6097 \pm j7.5635$	2.3893	0.3260
18	Gwagwa	$2.3576 \pm j8.1273$	0.3048	1.0640
19	Ikeja-West	$-0.5284 \pm j3.3182$	1.1601	0.2639
20	Ikot Ekpene	$4.6097 \pm j7.3637$	0.5060	0.2680
21	Jebba TS	$-1.7356 \pm j4.9214$	0.0931	4.6422
22	Jebba GS	$-1.7653 \pm j10.4192$	0.1311	0.1422
23	Jos	$1.4011 \pm j3.1375$	0.6534	0.3252
24	Kaduna	$-2.1746 \pm j6.7011$	0.7324	1.9180
25	Kainji GS	$-1.9640 \pm j5.3208$	0.6612	1.2912
26	Kano	$2.5376 \pm j10.9419$	0.3342	1.0768
27	Katampe	$-1.7011 \pm j3.1375$	0.3442	0.0768
28	Lokoja	$-2.1746 \pm j6.7011$	0.2632	0.7139
29	Makurdi	$-1.9640 \pm j5.3208$	0.6412	2.6122
30	New Haven	$2.0367 \pm j8.2287$	0.5941	0.6122
31	Okpai	$-3.4083 \pm j7.5374$	0.7456	5.4165
32	Olorunsogo	$0.2562 \pm j4.7324$	0.0674	3.4165
33	Omotosho	$2.7297 \pm j5.5635$	0.0384	4.2720
34	Onitsha	$0.4528 \pm j4.2183$	0.6259	0.1817
35	Osogbo	$-3.8372 \pm j6.3756$	0.1842	4.3366
36	Papalanto	$-2.7653 \pm j11.2419$	0.4933	0.3021
37	Sapele	$1.7301 \pm j3.1375$	0.2193	3.3021
38	Shiroro	$0.1674 \pm j4.1170$	0.0251	6.3228
39	Ugwuaji	$-1.6064 \pm j6.8320$	0.8232	3.1297
40	Yola	$-2.0367 \pm j8.2287$	1.7624	1.1096

3.3 Control of VSC-HVDC Transmissions

3.3.1 Topology and Training of ANN based regulator

The ANN regulator has two data inputs, one hidden layer and one output neuron; which is the easiest engineering variant since it comprises a single hidden layer. The input layer basically goes out as an input to the hidden layer where two neurons are utilized. The outputs are changed through a sigmoidal actuation capacity and took care of the output layer through their loads. The output layer has just a single neuron with a sigmodal actuation function. The inputs to the proposed ANN regulator (Fig. 2) are the reference current I_{ref} and estimated dc current I_{dc} and its output is the converter's thyristor terminating point (Renedo, García-Cerrada, Rouco and Sigrist, 2019). The error between I_{dc} and I_{ref} is utilized to adjust the weight of the ANN as per the delta rule. The speed of the controller and the system stability will depend on the learning rate η and the momentum μ used in adjusting the weights of the ANN.The ANN learns by adjusting the weights V_n and B_n in the hidden layer and the weights W_n and B in the output layer. (Lukowicz and Rosolowski, 2013)

International Journal of Advances in Engineering and Management (IJAEM)
Volume 4, Issue 2 Feb 2022, pp: 1397-1412 www.ijaem.net ISSN: 2395-5252

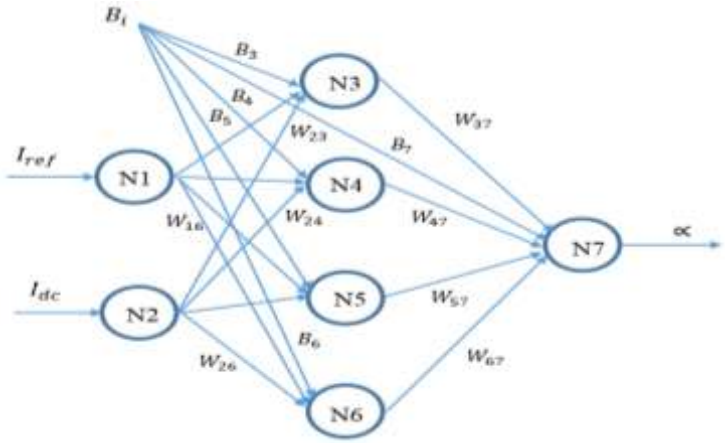

Figure 2: The typical Gaussian basis function neural network

The proposed ANN regulator comprises the accompanying three layers.

1. **Input layer:** In this layer, they are just two neurons, one of them is taken care of with a consistent reference current $I_{ref}$and the other neuron is I_{dc}.
2. **Hidden layer:** In this layer, there are (N) neurons. These are associated with the outputs of the input layer by weightsV_i, B_i, where i =1, …, N. The yields of these neurons are followed up on by the sigmoid capacity. The (N) outputs of the neurons in the hidden layer are taken care of to the yield layer through the weightW_i.
3. **Output layer:** This layer comprises one neuron in particular: the inputs to this neuron are the outputs from the hidden layer and the bias from the input layer. The weights and bias associated with these inputs are Wi and Bi, respectively. The information base that utilized for preparing neural network wanted current (I_{ref}) and real current (I_{dc}) as info, Tan-sigmoidal initiation work for covered up neurons, straight actuation work for yield neuron, number of cycles is 140 epoch, objective (error) 1e-5 and the output of neural network yield addresses the setting off point that applied on rectifier unit.

The ANN controller is trained Off-Line on the system data that obtained by traditional PI-controller, where the ANN controller is connected in parallel with PI controller as shown in Fig. 3.

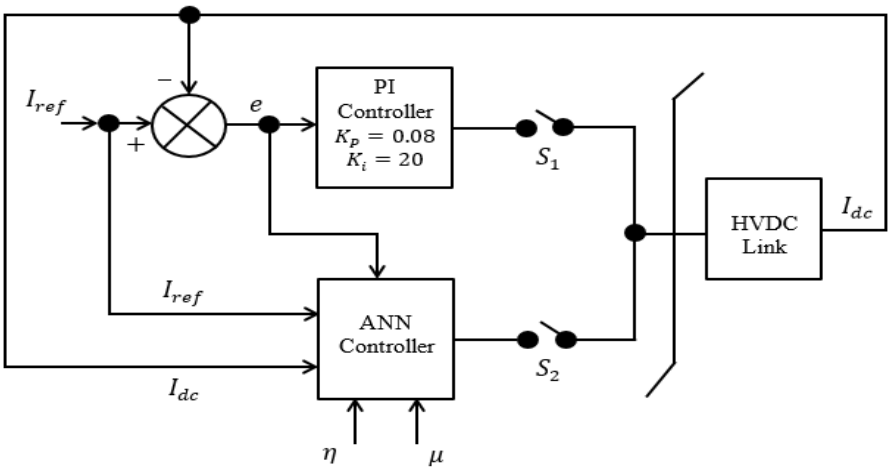

Figure 3: A schematic diagram of an HVDC system generic controller

After modeling the Multi Machine via VSC-HVDC system in which the detailed synchronous generator model was considered, the ANN controller was applied to the converter side to act on damping the synchronous machine power angle oscillations. This simple control guaranteed the reinforcement of the system dynamic performance and the power angle oscillations

International Journal of Advances in Engineering and Management (IJAEM)
Volume 4, Issue 2 Feb 2022, pp: 1397-1412 www.ijaem.net ISSN: 2395-5252

damping of the synchronous machine in presence of disturbances.

IV. INSTALLATION OF VSC-HVDC TO THE NETWORK DURING OCCURRENCE OF A THREE-PHASE FAULT

The HVDC system was installed on the two most critical buses in the Nigeria 330kV network. Load flow on the entire system was performed thereafter a three-phase fault was introduced on the same buses.A three-phase fault was created on the transmission lines connected to these two buses (very close to the buses) one after the other which forms the two scenarios. The swing equations are solved to obtain the network conditions for post-fault (see Section 3.1) using numerical solver ode45. The numerical solver, ode45, which is a built-in MATLAB/PSATS function, is employed in solving the m-number of swing equations within the system.

Figures 4 and 5 show the PSAT Model of the Nigeria 330kV transmission power system with VSC-HVDC installed along side with Omotosho – Benin and Shiroro – Jebba TS Transmission Lines respectively. The position for the location of the VSC-HVDC was determined through Eigen value analysis as aforementioned.After, the ANN control scheme was incorporated in the installedVSC-HVDC systemsand the entire process here in section 4 was repeated.

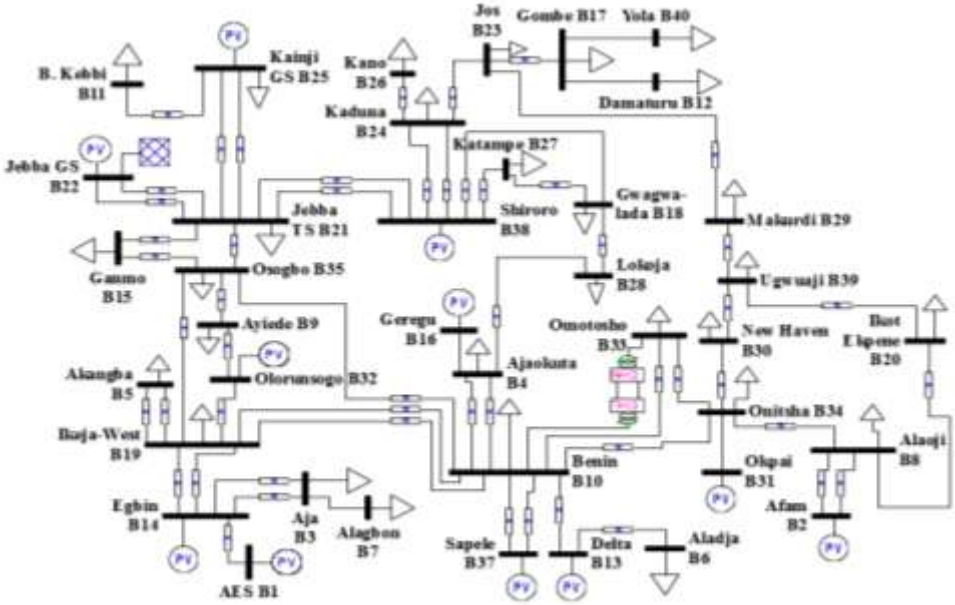

Figure 4:PSAT Model of the Nigeria 330kV transmission power system with VSC-HVDC installed along side with Omotosho – Benin Transmission Line

International Journal of Advances in Engineering and Management (IJAEM)
Volume 4, Issue 2 Feb 2022, pp: 1397-1412 www.ijaem.net ISSN: 2395-5252

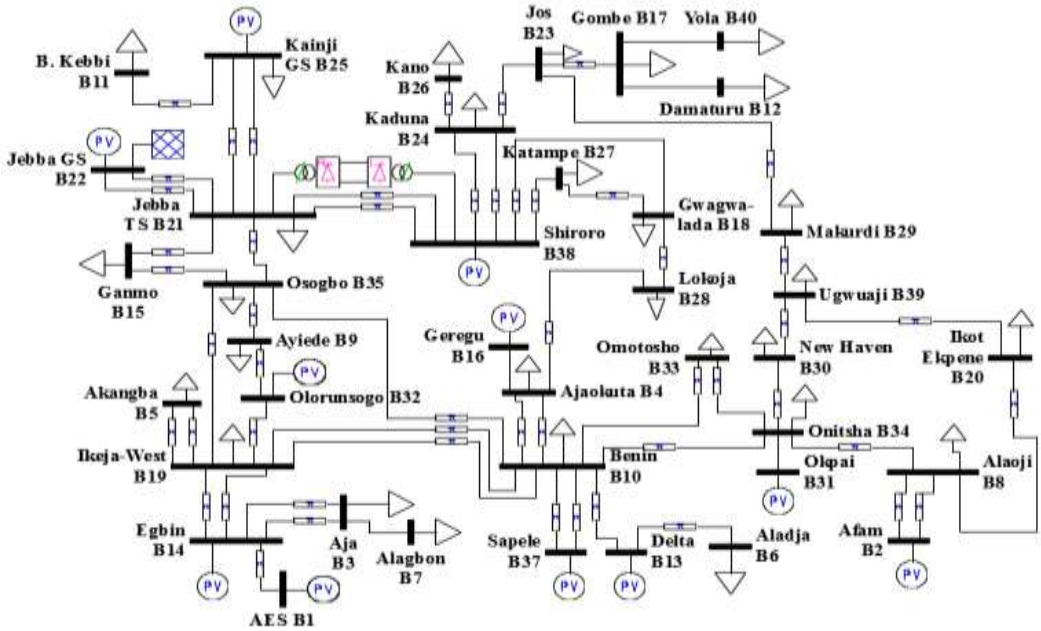

Figure 5: PSAT Model of the Nigeria 330kV transmission power system with VSC-HVDC installed along side with Shiroro – Jebba TS Transmission Line.

V. POWER FLOW ANALYSIS OF THE NIGERIA 40 BUS 330KV TRANSMISSION NETWORK

The Nigeria forty-bus 330kV transmission network voltage profile results are depicted in Figure6 as obtained from the power flow analysis of the network in PSAT environment. It can be observed from Figure 6 that the voltage magnitude at buses 5 (Akangba), 7 (Alagbon), 17 (Gombe), 18 (Gwagwalada), 26 (Kano), 32 (Olorunsogbo), 33 (Omotosho) and 38 (Shiroro) are below the acceptable voltage limit of ±10% for the Nigeria 330kV transmission network (Adepoju, Komolafe, Aborisade, 2011). This validates the findings of earlier researches on the system as detailed in (Ignatius and Emmanuel, 2017). Some of the system transmission lines have disproportionate power flows in them as depicted alighted in Table 2.

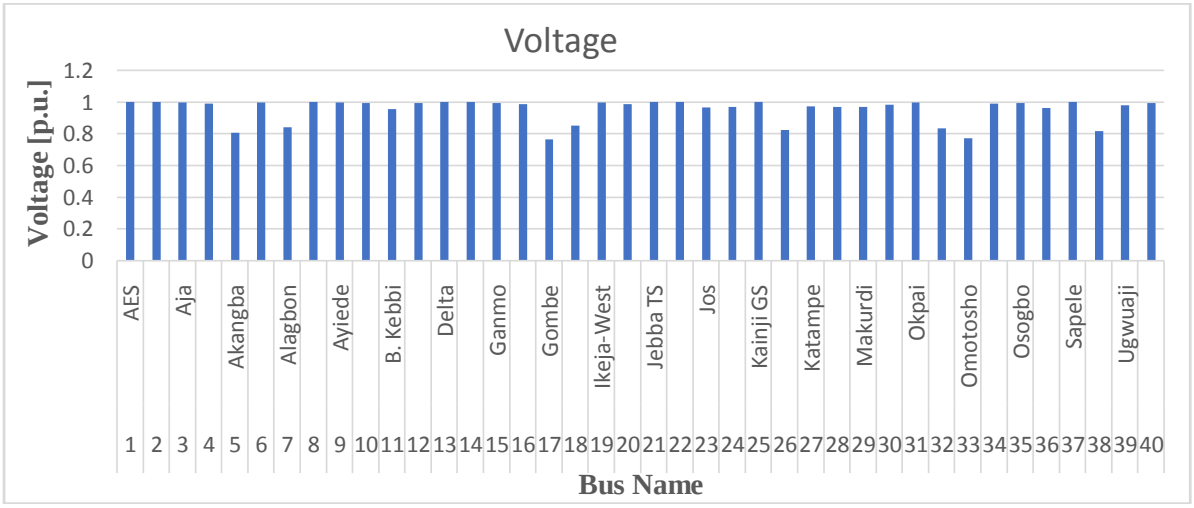

Figure 6:Nigeria 330kV Transmission Line Bus Voltage Profile

International Journal of Advances in Engineering and Management (IJAEM)
Volume 4, Issue 2 Feb 2022, pp: 1397-1412 www.ijaem.net ISSN: 2395-5252

VI. THE NETWORK RESPONSE TO OCCURRENCE OF A THREE-PHASE FAULT

The simulations were implemented on the MATLAB/PSAT environment. The demonstration for the transient stability analysis on the Nigeria 330-kV grid network, in this paper, considered two scenarios as aforementioned. These situations are made dependent on the Eigen values and the damping ratio of the buses. A three-phase fault was created on the transmission lines connected to the two buses,Omotosho and Shiroro buses (very close to the buses) one after the other which forms the two scenarios.and the swing equations are calculated to find the network conditions for both during-fault and post-fault using numerical solver ode45. The built-in MATLAB/PSATS function (in this case, the numerical solver, ode45), was used in solving the m-number of swing equations within the network (see Section 3.1).

6.1Scenario One: Three Phase Fault at Omotosho Bus

In this case, a three-phase fault was made on Omotosho bus (Bus 33) with line Omotosho – Benin (33-10) removed. Figures 7 and 8 show the dynamics responses of the generators for CCT of 300ms. Figures 7 and 8 show the plot of the power angle curves and the frequency responses of the eleven generators in the system during a transient three-phase fault on Omotosho to Benin transmission line respectively. It can be observed that generators at Olorunsogbo, AES, Geregu, Okpai, Afam, Delta and Sapele buses were most critically disturbed and failed to recover after the fault was cleared at 0.3seconds. These seven generators in the system lost synchronism and became unstable as shown in Figures 7 and 8.

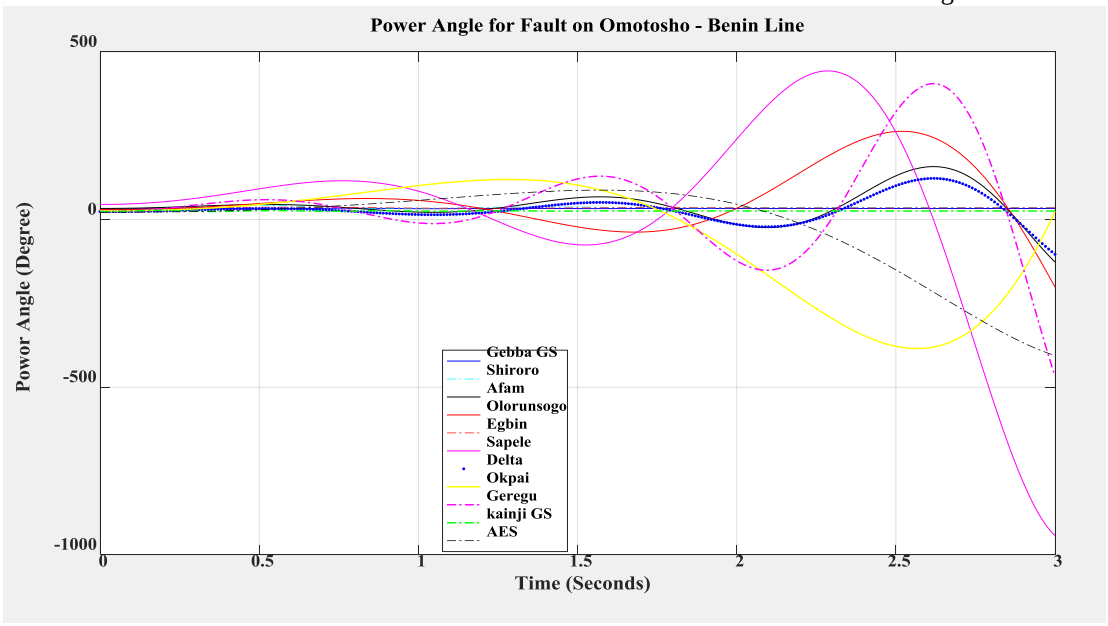

Figure 7:Power Angle response of the generators for fault clearing time of 0.3sec (without any VSC-HVDC)

International Journal of Advances in Engineering and Management (IJAEM)
Volume 4, Issue 2 Feb 2022, pp: 1397-1412 www.ijaem.net ISSN: 2395-5252

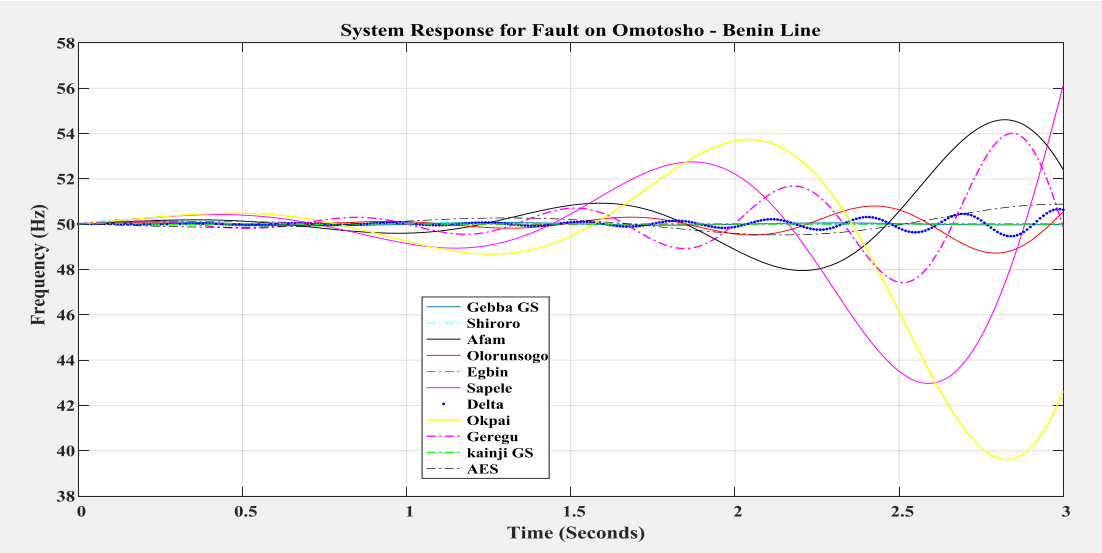

Figure 8:Frequency response of the system generators for fault clearing time of 0.3sec (without any VSC-HVDC)

The results of voltage profile of the Nigeria forty-bus 330kV transmission network after the occurrence of the fault are shown in Figure 9 as obtained from the power flow analysis of the network in PSAT environment. It can be observed from Figure 9 that there are serious voltage violations at buses 1 (AES), 2 (Afam), 13 (Delta), 16 (Geregu), 31 (Okpai), 32 (Olorunsogbo) and 37 (Sapele). The voltage magnitudes at these buses are lower than the acceptable voltage limit for the Nigeria 330kV transmission network.

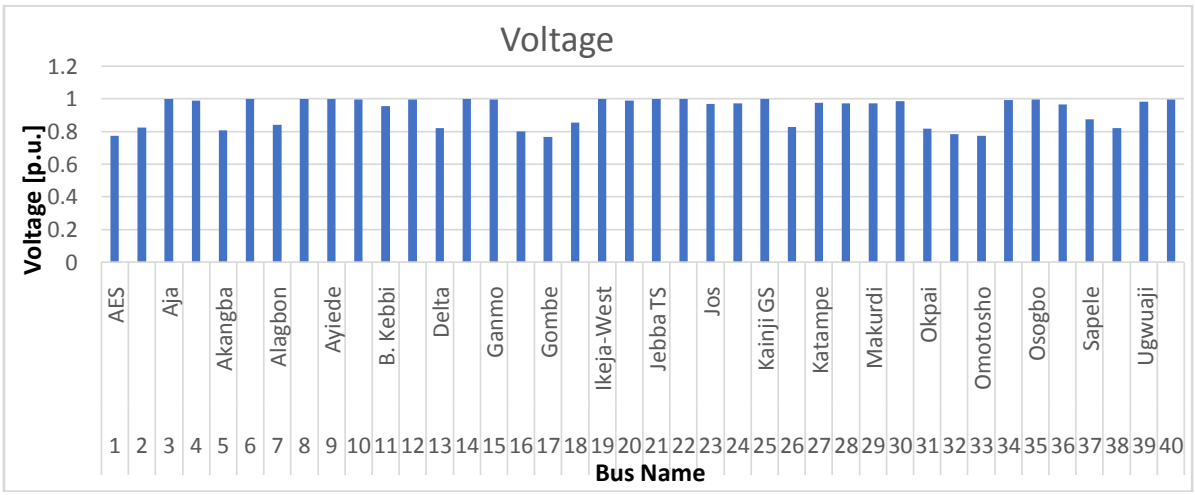

Figure 9:Nigeria 330kV Transmission Line Bus Voltage Profile during Occurrence of a Three Phase Fault on Omotosho Bus

6.2 Scenario Two: Three Phase Fault at Shiroro Bus

Again, a3-phase fault was made on Shiroro bus (Bus 38) with line Shiroro – Jebba TS (38 - 21) removed by the circuit breakers (CBs) at both ends opening to remove the faulted line from the system. Figures 10 and 11 show the generators dynamics responses for CCT of 300ms. Figures 10 and 11 show the plot of the power angle curves and the frequency responses of the eleven generators in the system during a transient three-phase fault on Shiroro to Jebba TS transmission line respectively. It can be observed that virtually all generators in the system at were critically disturbed and all failed to recover after the fault was cleared at 0.3seconds. So, the system lost synchronism and became unstable.

International Journal of Advances in Engineering and Management (IJAEM)
Volume 4, Issue 2 Feb 2022, pp: 1397-1412 www.ijaem.net ISSN: 2395-5252

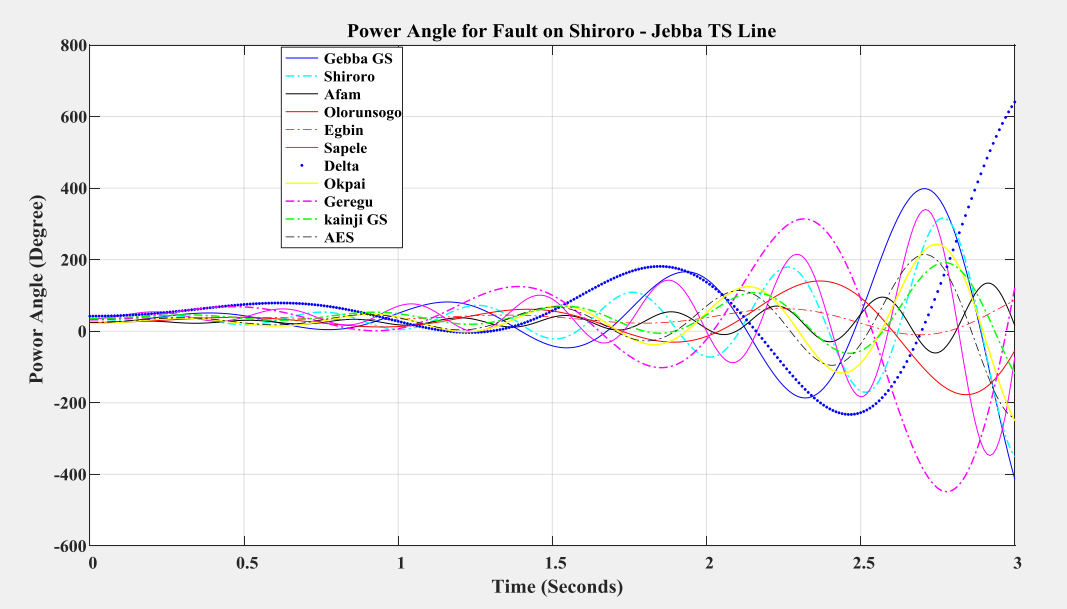

Figure 10:Power Angle response of the generators for fault clearing time of 0.3sec (without any VSC-HVDC)

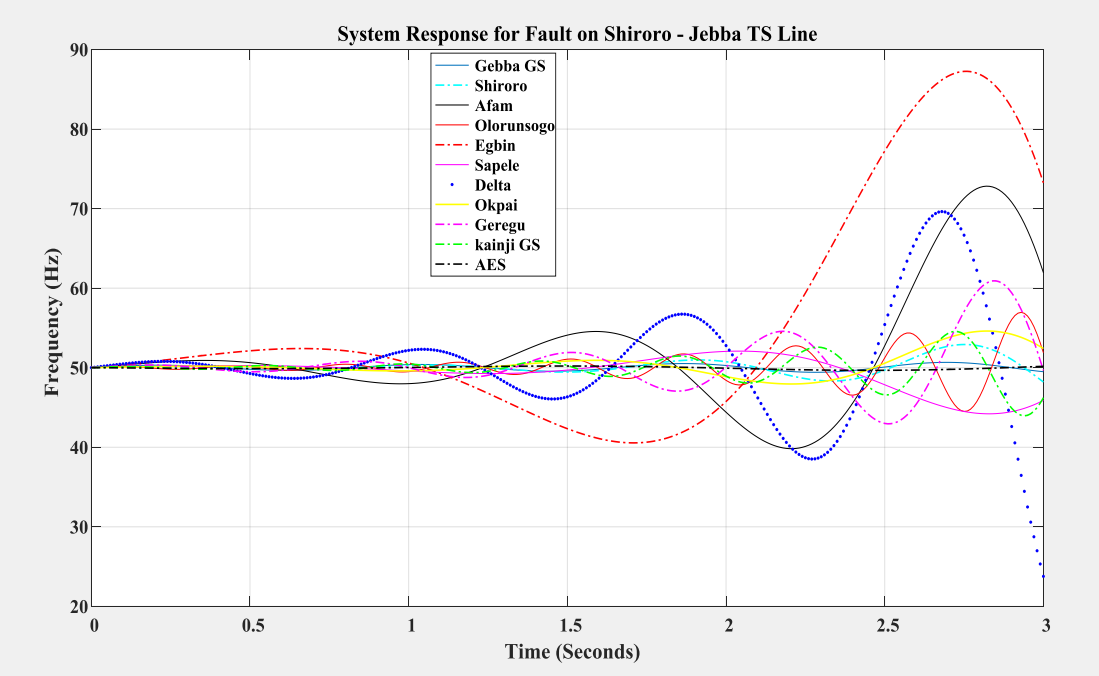

Figure 11:Frequency response of the system generators for fault clearing time of 0.3sec (without any VSC-HVDC)

VII. THE GRID RESPONSE TO OCCURRENCE OF A THREE-PHASE FAULT WITH ANN CONTROLLED VSC-HVDC INSTALLED AT THE UNSTABLE BUSES

Here, ANN was used to regulate and control the parameters of the rectifier and the inverter of the VSC-HVDC instead of the convectional PI method. The idea is to see the effect of the HVDC, whose parameters are being controlled by neural network, on the transient stability of the system during occurrence of a three-phase transient fault and also on the bus voltage violations. The effect of the control strategy on

International Journal of Advances in Engineering and Management (IJAEM)
Volume 4, Issue 2 Feb 2022, pp: 1397-1412 www.ijaem.net ISSN: 2395-5252

transient stability has been quantified with the critical clearing time (CCT).

It is important to state again, that the maximum allowable time that a disturbance can stay until it is cleared, without resulting to loss of synchronism is known as the critical clearing time (CCT). It is usually employed as a transient stability margin indicator.

7.1. Scenario One: Three Phase Fault at Omotosho Bus

As before, a three-phase fault was initiated on Omotosho bus (Bus 33) with line Omotosho – Benin (33-10) removed by the CBs at both ends opening to remove the faulted line from the system. Figures 12 and 13 show the plot of the power angle curves and the frequency responses of the eleven generators in the system during a transient three-phase fault on Omotosho to Benin transmission line respectively. It can be observed that oscillation of those seven generators at Geregu, Afam, Olorunsogbo, Opkai, AES, Delta and Sapele buses which were most critically disturbed during a fault occurrence without VSC-HVDC, along with other buses have achieved faster damping. It can also be noted that the CCT has been increased from 300milli-seconds to 450milli-seconds and also the oscillations were quickly damped compare to the results obtain when the VSC-HVDC was being controlled by the conventional PI method.

This, again can be attributed to the intelligent response of the neural network in controlling the parameters of the VSC-HVDC, which enabled to inject the needed power in the two buses (Bus 33 – 10) in time and most appropriately. Hence, from Figures 12 and 13, the transient stability of the system has been further improved with the intelligent HVDC in the system.

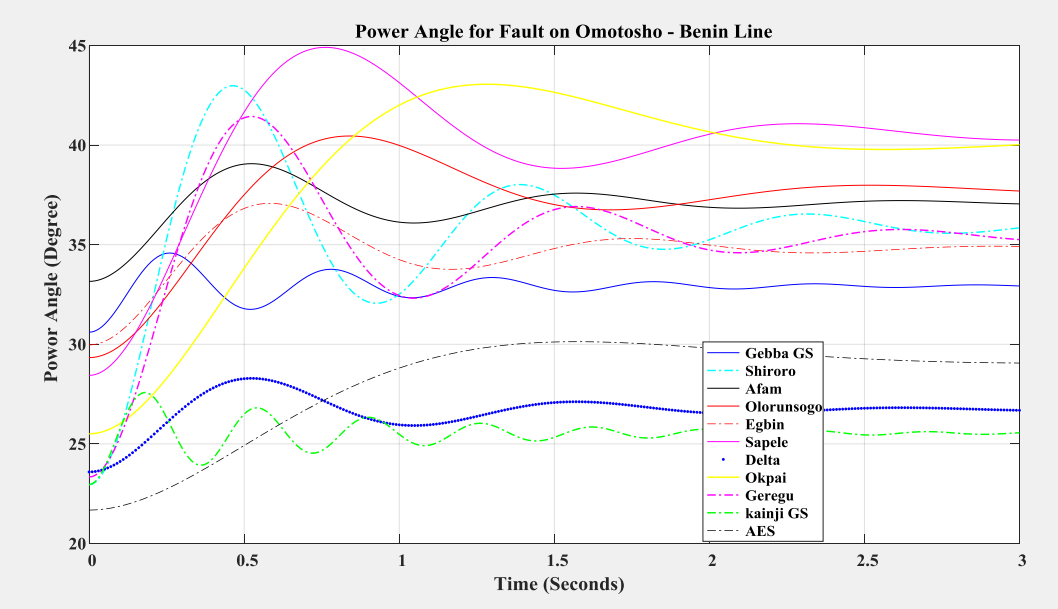

Figure 12:Power Angle response of the generators for fault clearing time of 0.45sec (with ANN Controlled VSC-HVDC)

International Journal of Advances in Engineering and Management (IJAEM)
Volume 4, Issue 2 Feb 2022, pp: 1397-1412 www.ijaem.net ISSN: 2395-5252

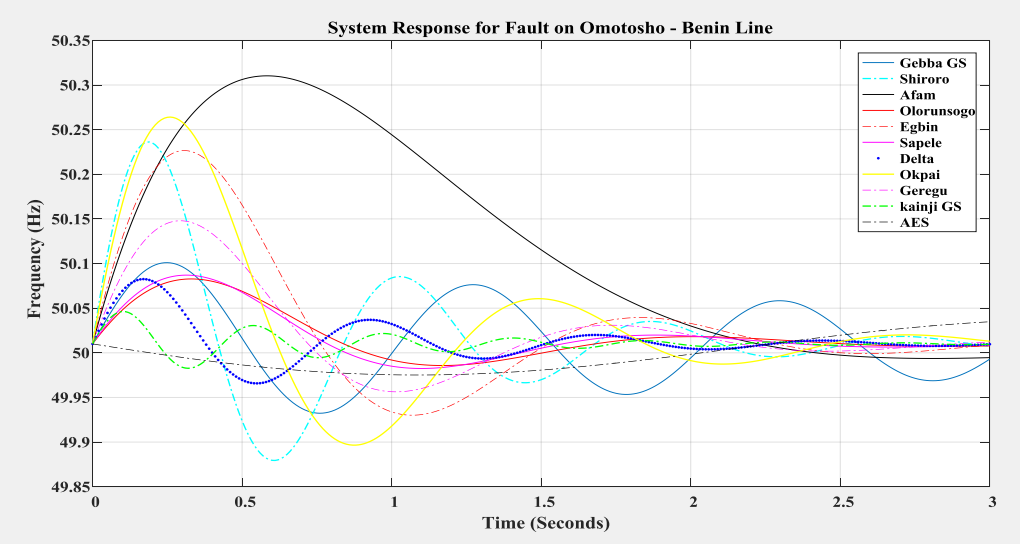

Figure 13:Frequency response of the system generators for fault clearing time of 0.45sec (with ANN Controlled VSC-HVDC)

The results of the voltage profile of the 40-bus Nigeria 330kV grid with ANN Controlled VSC-HVDC installed between Omotosho to Benin bus after the occurrence of the fault are shown in Figure 14 as obtained from the power flow analysis of the network in PSAT environment. It can be observed from Figure 4.24 that the voltage violations at buses 1, 2, 13, 16, 31, 32 and 37 which were 0.905738, 0.909903, 0.922923, 0.919679, 0.941849, 0.919188 and 0.960770 as obtained previously when there was no VSC-HVDC were improved to 0.998421, 1.000000, 0.999275, 0.979914, 0.997805, 0.998835 and 1.000000 respectively. This is as result of the intelligent response of the VSC-HVDC in injecting adequate reactive power timely.

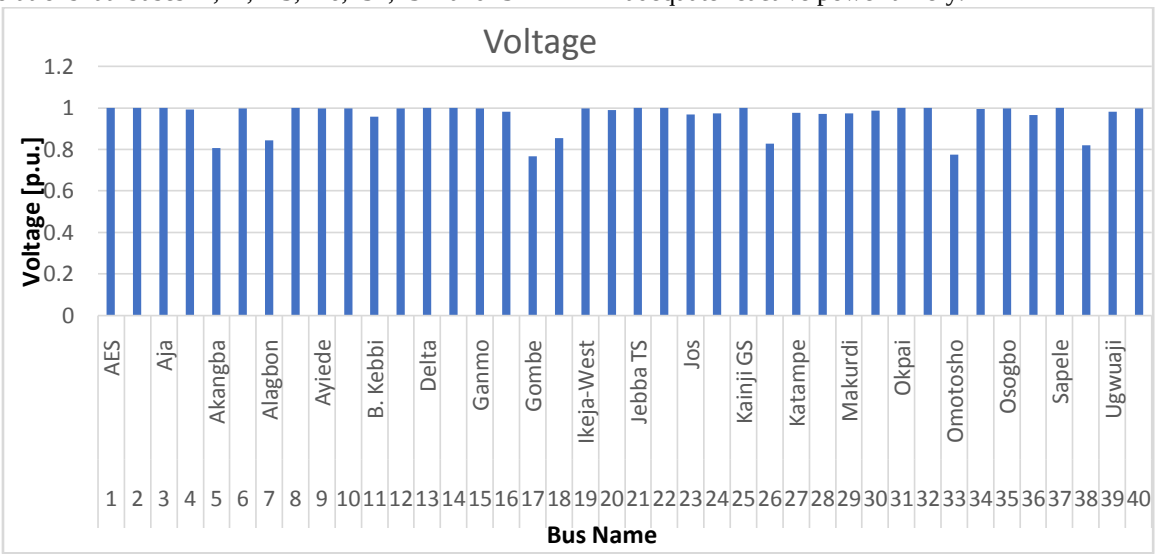

Figure 14:Nigeria 330kV Transmission Line Bus Voltage Profile during Occurrence of a Three Phase Fault on Omotosho Bus with ANN Controlled VSC-HVDC Installed

7.2.Scenario Two: Three Phase Fault at Shiroro Bus

As before, a three-phase fault was initiated at Shiroro bus (Bus 38) with line Shiroro – Jebba TS (38 - 21) removed by the CBs at both ends opening to remove the faulted line from the system. Figures 15 and 16 show the plot of the power angle curves and the frequency responses of the eleven generators in the system during a transient three-phase fault on Shiroro to Jebba TS transmission line. It can be observed that all the generators in the system which were all critically disturbed during a

International Journal of Advances in Engineering and Management (IJAEM)
Volume 4, Issue 2 Feb 2022, pp: 1397-1412 www.ijaem.net ISSN: 2395-5252

fault occurrence without VSC-HVDC, have achieved faster damping. It can also be noted that the CCT has been increased from 300milli-seconds to 450milli-seconds and also the oscillations were quickly damped compare to the results obtain when the VSC-HVDC was being controlled by the conventional PI method.

This, again can be attributed to the intelligent response of the neural network in controlling the parameters of the VSC-HVDC, which enabled to inject the needed power in the two buses (Bus 38 – 21) in time and most appropriately. Hence, the transient stability of the system has been further improved with the intelligent HVDC in the system.

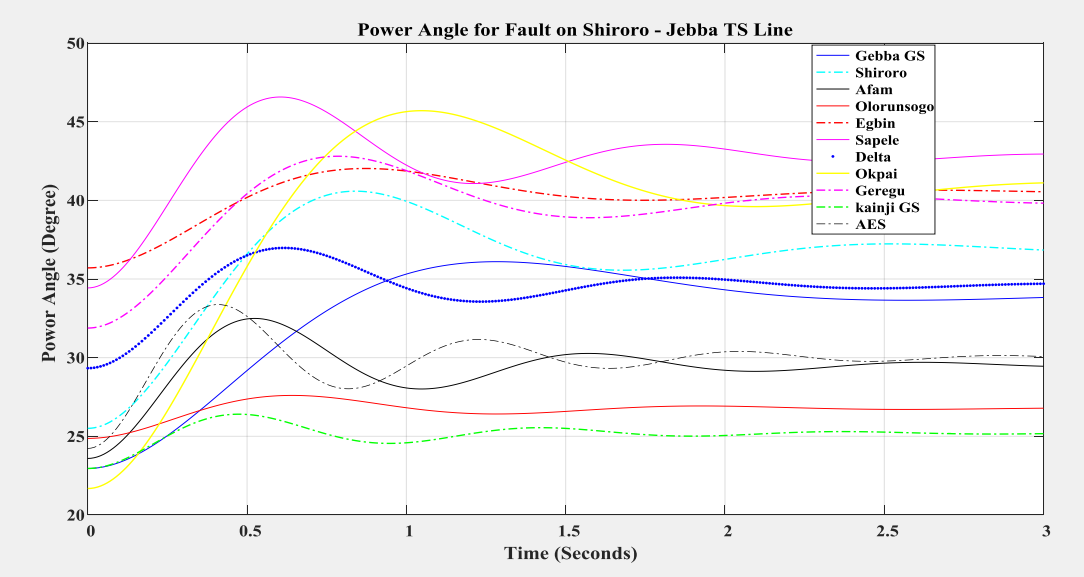

Figure 15:Power Angle response of the generators for fault clearing time of 0.45sec (with ANN Controlled VSC-HVDC)

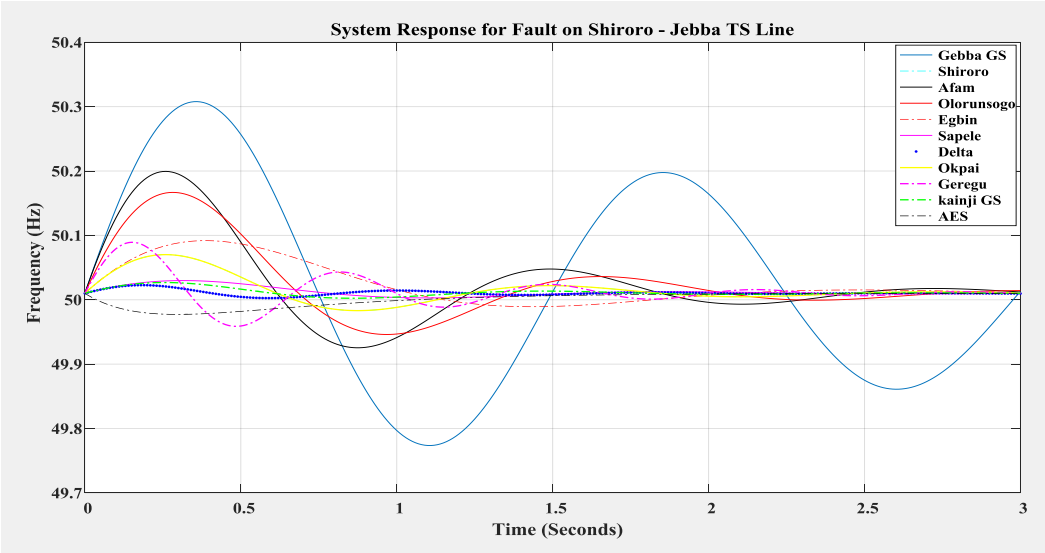

Figure 16:Frequency response of the system generators for fault clearing time of 0.45sec (with ANN Controlled VSC-HVDC)

The results of the voltage profile of the 40-bus Nigeria 330kV grid with ANN Controlled VSC-HVDC installed between Shiroro to Benin bus after the occurrence of the fault as obtained from the power flow analysis of the network in PSAT environment shows that the voltage violations at buses 1, 2, 13, and 37 which were 0.930561,0.905654,0.922923 and 0.920670 as obtained previously when there was no VSC-HVDC were all improved to 1.000000p.u. each

while the voltages at buses 16, 31, 32 remained the same. This is as result of the intelligent response of the VSC-HVDC in injecting adequate reactive power timely.

VIII. CONCLUSIONS

Some result findings that were established are as follows:

i) The Eigen value analysis revealed that most buses in the network are generally not stable (as can be seen from Table 4.1) which makes the Nigerian 330kV transmission grid marginally unstable.
ii) It was also shown thatbus Omotosho (bus 33) and bus Shiroro (bus 38) are buses with lowest damping ratio. Coupled with the fact that the eigenvalues of these buses are located on the right side of the S-plane, it makes them the most unstable.
iii) It was established that the Nigerian 330kV transmission network had no transient stability compensation technology incorporated in it. Not even FACTS devices.
iv) It was established that the transient stability of Nigerian 330kV transmission network could be improved using ANN controlled VSC-HVDC.

The dissertation has successfully implemented that the transient stability of the Nigeria 330kV transmission network can be significantly enhanced by applying an intelligent HVDC to the network. This has allowed the case study network (the Nigerian 330kV Power transmission line) to receive simulation procedures and results peculiar and specific to its parameters. The HVDC has its inverter and converter parameters controlled using artificial neural network instead of the conventional PI controller. The eminent system collapse of the Nigeria 330kV transmission network as a result of the system being marginally unstable has been mitigated by this dissertation.

IX. RECOMMENDATION

Support Vector Machine (SVM) could also be used instead of ANN to control the VSC-HVDC for enhancement of the transient stability of the Nigeria 330kV network. The CCT obtained could be compared to that of ANN controlled VSC-HVDC. Considering the unstable nature of Nigeria 330kV grid system as analyzed and the significant impact of the ANN HVDC link in improving the transient stability of the network, it will be wise to recommend the installationof the HVDCs in the three most critical buses as aforementioned having seen the magnificent improvement.

REFRENCES

[1]. Ayodele T R, Jimoh A. A., Munda J. L., and Agee J T, (2012). The impact of wind power on power system transient stability based on probabilistic weighting method. Journal of Renewable and Sustainable Energy, 4, 1-18.
[2]. Ayodele T. R., Ogunjuyigba A. S. O. and Oladele O. O., (2016). Improving the Transient Stability of Nigerian 330kV Transmission Network using SVC, Nigeria Journal of Technology, pp. 155-166.
[3]. Eleschová Ž., Smitková M. and Beláň A. (2010). Evaluation of Power System Transient Stability and Definition of the Basic Criterion. International Journal of Energy, Issue 1, Vol. 4.
[4]. Eriksson R. (2014). Coordinated Control of Multiterminal DC Grid Power Injections for Improved Rotor-Angle Stability Based on Lyapunov Theory. IEEE Transactions on Power Delivery, Vol.29, No.4, pp.1789–1797.
[5]. Hua L., Tian-gang Y., Mu-Zi Z., Zhi-min L. (2012). HVDC Intelligent Controller. International Conference on Future Electrical Power and Energy Systems. © Published by Elsevier Ltd; Energy Procedia 17pp 1460 – 1467
[6]. Ignatius K. O., Emmanuel A. O. (2017). Transient Stability Analysis of the Nigeria 330-kV Transmission Network. American Journal of Electrical Power and Energy Systems; 6(6): 79-87,http://www.sciencepublishinggroup.com/j/epes,doi:10.11648/j.epes.20170606.11; ISSN: 2326-912X (Print); ISSN: 2326-9200 (Online)
[7]. Karthikeyan K. and Dhal P. K. (2015). Transient Stability Enhancement by Optimal location and tuning of STATCOM using PSO. Smart and Grid Technologies (ELSEVEIR), pp. 340-351.
[8]. Lukowicz M., Rosolowski E. (2013). Artificial neural network based dynamic compensation of current transformer errors. Proceedings of the 8th International Symposium on Short-Circuit Currents in Power Systems, Brussels, pp. 19-24.
[9]. Machowski J., Kacejko P., Nogal L. and Wancerz M. (2013). Power system stability enhancement by WAMS-based supplementary control of multi-terminal HVDC networks. Control Engineering Practice, Vol.21, No.5, pp.583–592.
[10]. Mohapatra B. K. S. (2015). Dynamic Stability Improvement of Power System

with VSC-HVDC Transmission. A Thesis submitted to the Department of Electrical Engineering, National Institute of Technology, Rourkela, Rourkela-769008, India. http//:www.nitrkl.ac.in

[11]. Renedo J., García-Cerrada A., Rouco L. and Sigrist L. (2019). Coordinated Control in VSC-HVDC Multi-Terminal Systems to Improve Transient Stability: The Impact of Communication Latency. Energies 12, 3638; doi:10.3390/en12193638.www.mdpi.com/journal/energies

[12]. Sharma P. R. and Hooda, (2012). Transient Stability Analysis of Power System using MATLAB. International Journal of Engineering Sciences and Research Technology, pp. 418-422

[13]. Sravani, T., Hari, G. and Basha, J. (2010). Improvement of Power System Stability Using SFCL in Elastic Power Grid under Voltage Unbalance Conditions. International Journal of Emerging Trends in Electrical and Electronics, 10, 80-89.

[14]. Srinvasa, J. and Amarnath, J. (2014). Enhancement of transient Stability in a deregulated Power System Using FACTS Devices. Global Journal of Researches in Engineering, 14, 1-17.